

Citation for published version:
Ahmet, IY, Hill, MS, Johnson, AL & Peter, LM 2015, 'Polymorph-Selective Deposition of High Purity SnS Thin Films from a Single Source Precursor', Chemistry of Materials, vol. 27, no. 22, pp. 7680-7688. https://doi.org/10.1021/acs.chemmater.5b03220

10.1021/acs.chemmater.5b03220

Publication date: 2015

Document Version Early version, also known as pre-print

Link to publication

University of Bath

Alternative formats

If you require this document in an alternative format, please contact: openaccess@bath.ac.uk

Copyright and moral rights for the publications made accessible in the public portal are retained by the authors and/or other copyright owners and it is a condition of accessing publications that users recognise and abide by the legal requirements associated with these rights.

Take down policyIf you believe that this document breaches copyright please contact us providing details, and we will remove access to the work immediately and investigate your claim.

Download date: 12. Mar. 2023

Polymorph-Selective Deposition of High Purity SnS Thin Films from a Single Source Precursor

Ibbi Y. Ahmet,^{†‡} Michael S. Hill,[†] Andrew L. Johnson*[†] and Laurence M. Peter.[†].

†Department of Chemistry, University of Bath, Bath, BA2 7AY, United Kingdom. ‡Centre for Sustainable Chemical Technologies, University of Bath, Bath, BA2 7AY, United Kingdom.

Content

<u>Information</u>	<u>Page</u>
Schematic of AA-CVD Reactor	S2
Photo Electrochemical Measurements	S3-6
a) Sample Preperation	S3
a) Photoelectrochemical Cell	S3
c) Photo current under single wavelength LED	S3-4
illumination	
d) Photocurrent spectroscopy	S4-5
e) Calculating the EQE of a photocurrent spectrum	S5
e) Calculating the expect Jsc of a sample	S5
Diagrams of Photoelectrochemical Devices	S 6
Synthetic Methedology	S7-9
Synthesis of Tetrakis(dimethylamido)ditin(II)	S7
Synthesis of Dimethylamido-(N-Phenyl-N',N'-	S8
Dimethyl-Thiouriate)Sn(II) dimer	
Photograph of compound (1)	S9
¹¹⁹ Sn, ¹³ C and ¹ H NMR Data of Compound (1)	S10
¹³ C and ¹ H NMR Data for the By-Product Solution	S11
Photographs of Films	S12
Additional SEM images	S13
Energy Dispersive X-ray Spectroscopy (EDAX) Data	S14
X-ray Photoelectron Spectroscopy (XPS) Data	S15-16
Thermogravimetric Analysis (TGA) of Compound (1)	S17
Optical Data	S18
Additional Photocurrent and External Quantum Efficiency	
(EQE) Spectrum	S19
Addition Powder X-ray Diffraction (PXRD) Spectrum	S20
Single Crystal X-ray Diffraction Data for Compound (1)	S21-22
References	S23

Aerosol Assisted- Chemical Vapour Depositions (AA-CVD) were performed on the in-house designed apparatus displayed and labelled below:

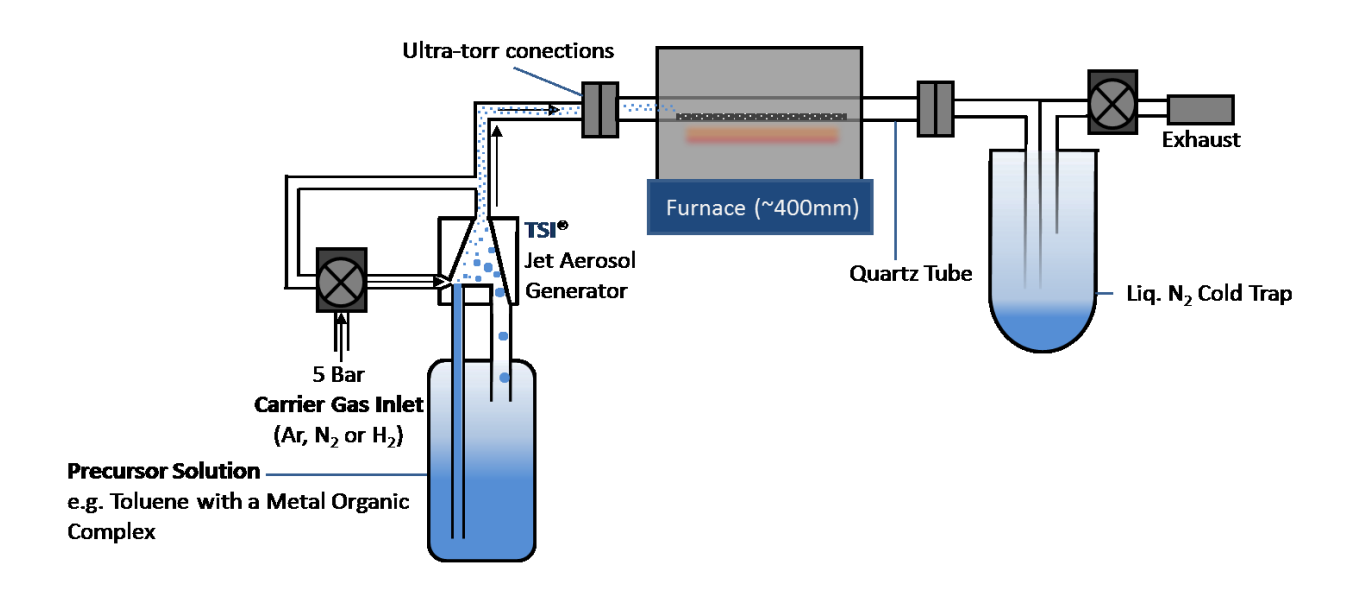


Figure S.1: Schematic of the AA-CVD reactor.

Photoelectrochemical measurements:

a) Sample Preparation

SnS was deposited onto Molybdenum substrates (1 cm by 3.5 cm) using the specified AACVD precursor and techniques. The SnS film was removed from the end section of the sample (c.a. 1 cm by 0.7 cm area) by abrasion with 1 µm alumina paste to expose the Mo back contact which was then painted with RS Standard Silver contact paint and connect to the Potentiostat with crocodile clips. The edges of the samples were isolated by scribing through the film with a diamond tipped stylus, and the area (c.a. 1 cm by 1cm) to be measured was delineated with polyimide tape.

b) The Photoelectrochemical Cell

The measurement cell was a glass-sided vessel with approximate volume of 27 cm³ (3cm by 3cm). All photoelectrochemical measurements on SnS films were carried out using an aqueous solution of 0.2 M Eu(NO₃)₃.6H₂O (99.9%, Alfa Aesar) as an electron-scavenging redox electrolyte. The photocurrent responses of the films were measured under potentiostatic control (synchronised with the chopper frequency or Flashing LED) using Pt wire counter and Ag|AgCl reference electrodes.

c) Photo current under single wavelength LED illumination (Measurements for Chronoamperometry and Flashing Sweep)

Photo current under single wavelength LED illuminations were measured using the setup shown in **Figure S3**. All measurement were conducted in a Faraday cage to eliminate external electromagnetic interference and illumination. Transient photocurrents were generated using a constant or pulsed illumination from a ThorLabs LEDC8-Collimated 470nm LED ~10 cm from the sample surface and measured using an Ivium Compactstat potentiostat at a range of

potentials against an Ag|AgCl reference electrode. Data was recorded on IviumSoft Electrochemistry Software.

- 1) Chronoamperometry measurements where conducted at fixed potentials of -0.6 V or +0.6 V for a duration of 60 sec. Before measurements were under taken the sample was kept in the dark at the measurement potential for 30 seconds to allow the system to reach equilibrium. The blue 470 nm LED was used and pulsed for 1.5 sec on and 0.5 sec off.
- 2) Flashing Sweep measurements were conducted by flashing the 470 nm LED on for 1 s and off for 1 s with a sweeping potential from -0.7 V to +0.7 V at 0.02 V per second.

d) Photocurrent spectroscopy (Measurement of External Quantum Efficiency [EQE])

The sample cell and battery-powered potentiostat were placed within a Faraday cage to eliminate external electromagnetic interference and illumination. Photocurrent spectra were obtained using monochromatic light of variable wavelength provided by a tungsten argon lamp (IL6S Bentham Illumination), grating monochromator (G312 ROUG grating) and stepper controller (Bentham PCM3B/IEEE), which was calibrated and controlled using the LabVIEW software. The incident light was chopped at 27 Hz and a current amplifier (Femto DLPCA-200) both connected to a lock-in amplifier (Stanford Research Systems ST830 DSP) was used to detect the photocurrent. A yellow filter was used to remove second-order harmonics from the monochromated light at wavelengths above 550 nm. Measurements of the photocurrent as a function of wavelength were made at a potential of -0.7 V and +1.0 V vs. Ag|AgCl, using a home built battery powered DC potentiostat. The spectrum was recorded twice in opposite directions for wavelength to confirm that the sample was stable before performing a slower scan to record the final spectrum. Measurements in the range 1100-400 nm were performed with 10 nm intervals. In order to obtain the external quantum efficiency (EOE) of the SnS films.

the incident photon flux was calibrated using standardized 1 cm² Si photodiode traceable to NBS standards. The after all EQE measurements photo current measurements as a function of wavelength were recorded using the Si photodiode in order to calibrate the spectral flux produced by the tungsten lamp, which is used in the calculations of the EQE.

e) Calculating the EQE of a photocurrent spectrum

To determine an EQE of a sample, we simply measure the photocurrent produced at different photon energies and calibrate the data to the photocurrent produced by a photodetector, which has a known EQE spectrum. Using the following expression, this allows us to determine the photocurrent of a sample, using this device set-up:

$$\Phi_S = \Phi_{pd} \frac{\Delta J_S}{\Delta J_{pd}}$$

Where ϕ is photo energy depend the EQE, ΔJ is the photo current produced across a small range of photon energies and the subscripts 'S' and 'pd' refer to the sample and the photodiode respectively. Therefore by dividing the photocurrent generated by the sample by the photocurrent generated by the photodiode at specific photon energies. Then multiplying this value by the EQE value of the photodiode at this photon energy, the EQE of the sample at specific photon energies can be determined.

f) Calculating the expect J_{sc} of a sample under standard conditions:

The J_{sc} of a sample under standard conditions can be calculated by integrating the EQE spectrum multiplied by spectral photon flux density (m⁻²s⁻¹eV⁻¹), b(E), of AM 1.5 G, as shown below:

$$J_{sc} = q \int_0^\infty \Phi(E) b(E) dE$$

Where J_{sc} is the short circuit current density, q is the electronic charge (±1), E is the photon energy (nm or eV) and ϕ sample EQE ¹.

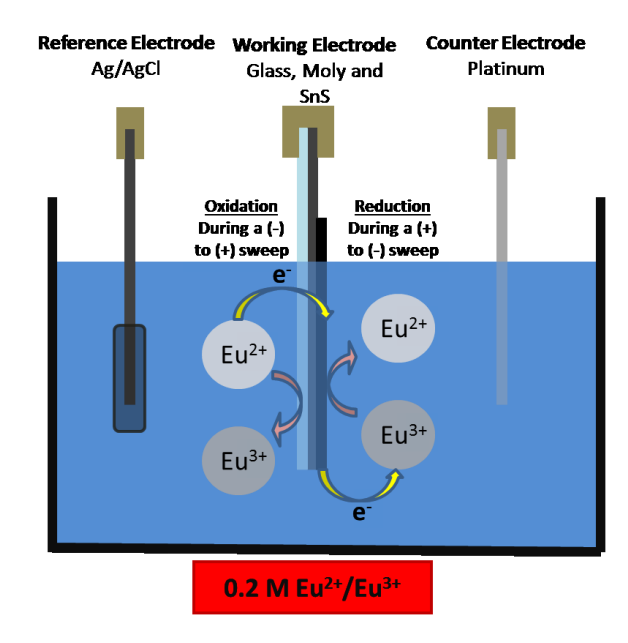


Figure S2: Diagram of the Photoelectrochemical Cell.

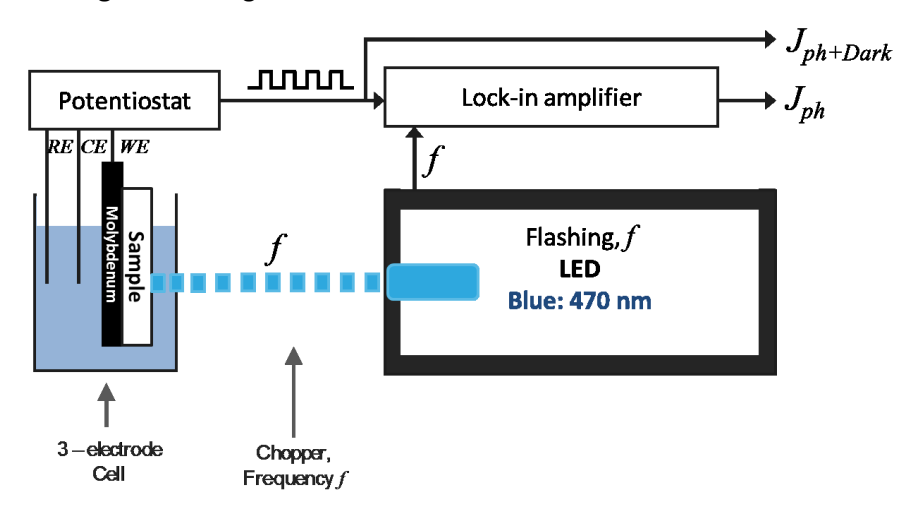


Figure S3: Diagram of device setup for photocurrent measurements under single wavelength LED.

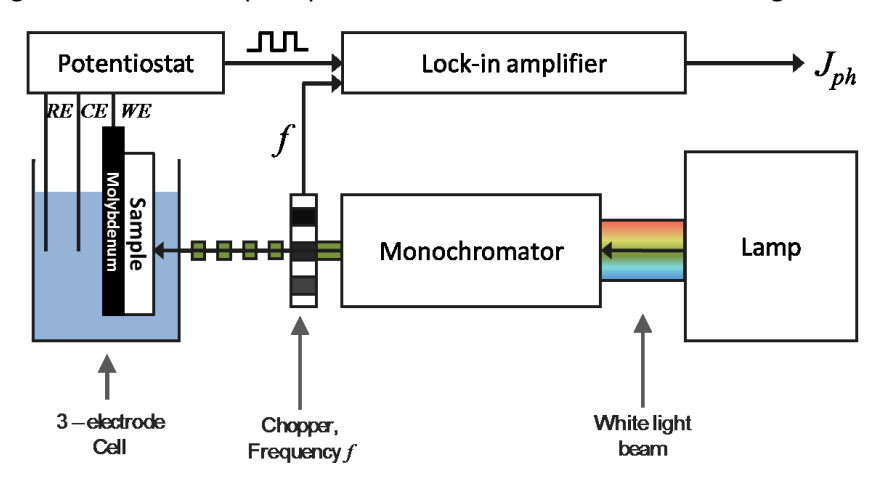


Figure S4: Diagram of device setup for photocurrent current spectroscopy for EQE measurements.

Synthesis of Tetrakis(dimethylamido)ditin(II) [Sn(NMe2)2] (Reagent 1):

Tetrakis(dimethylamido)ditin(II) was synthesized as previously described ², from lithium dimethyl amide and anhydrous tin(II) chloride (Purchase from Sigma Aldrich).

Cooled at -40 °C, a stirred diethyl ether (200 ml) mixture of anhydrous tin(II) dichloride (18.90 g, 0.1 mol) was treated with a cooled diethyl ether (400 ml) slurry of lithium dimethyl amide (10.18g, 0.2 mol) via cannula transfer. The mixture was allowed to slowly react room temperature and stirred for 24 hours where a white precipitate and orange solution was formed. Diethyl ether was removed *in vacuo* and the remaining solid was treated with 400 ml of hexane and stirred for 1 hour. The white precipitate was removed via silica frit filtration with celite aid to generate a clear yellow solution. The solution was reduced by three quarters by *in vacuo* and cooled to 0 °C to generate the product as colourless crystalline plates. The product was subsequently separated by filtration and dried under vacuum. Yield 19.4 g, 94 %. m.p. 91 °C. Analysis, found (calc. for C₄H₁₂N₂Sn): C 23.01 (23.22); H 5.77 (5.85); N 13.55 (13.54). ¹H NMR (300 MHz, C₆D₆): δ_H 2.80 (br s, 12H, N(CH₃)). ¹³C {¹H} NMR (75.5 MHz, C₆D₆): δ_C 43.23 (s, NCH₃). ¹¹⁹Sn {¹H} NMR (95.3 MHz, C₆D₆): δ_{Sn} 122.73 (s).

Synthesis of Dimethylamido-(N-Phenyl-N',N'-Dimethyl-Thiouriate)Sn(II) dimer [Sn({C₆H₅}NCSN{Me₂})(NMe₂)] Compound (1):

Phenylisothiocyanate (2.40 ml, 2.276 g, 20.10 mmol) was added drop wise, over 10 minutes, to a cooled (-40 °C) and stirred THF solution (100 ml) of tetrakis(dimethylamido)ditin(II) (4.180 g, 20.10 mmol) which resulted in an instantaneous colour change from yellow to colourless. After stirring at room temperature for 2 hrs, THF was removed *in-vacuo*. To the residual solid 80 ml of hexane was added and stirred for 1 hour, where-upon a white precipitate evolved. The hexane was removed from the precipitate by cannula filtration. The precipitate was washed a further two times with fresh hexane. The white precipitate was then dissolved in a THF:hexane mix (15ml:30 ml). After filtration through celite, the solution was stored at -20 °C for 3 days, during which time colourless crystalline needles were formed. The product was subsequently isolated by filtration and dried *in-vacuo*. Yield 5.552 g, 86 %, m.p. 125 °C decomposed to black. Analysis, found (calc. for C₁₁H₁₇N₃SSn): C 38.40 (38.63); H 5.35 (5.01); N 12.15 (12.29). ¹H NMR (300 MHz, THF-d⁸): δ_H 7.20-7.11 (m, 2H, N(C₆H₅)), 6.91-6.72 (m, 3H, N(C₆H₅)), 2.83 (s, 6H, N(CH₃)), 2.62 (s, 6H, N(CH₃)). ¹³C NMR (75.5 MHz, THF-d⁸): δ_C 129.43 (s, N-C(=S)-N),123.23 (s, N(C₆H₅)), 45.37 (s, N(CH₃)), 42.13 (s, N(CH₃)). ¹¹⁹Sn NMR (111.95 MHz, THF-d⁸): δ_{Sn 38.50} (s).

$$\begin{array}{c} \text{THF} \\ \text{Me}_2 \text{N} \\ \text{Me}_2 \text{N} \end{array} + \text{S} = \text{C} = \text{N} \\ \begin{array}{c} \text{Me}_2 \text{N} \\ \end{array}$$

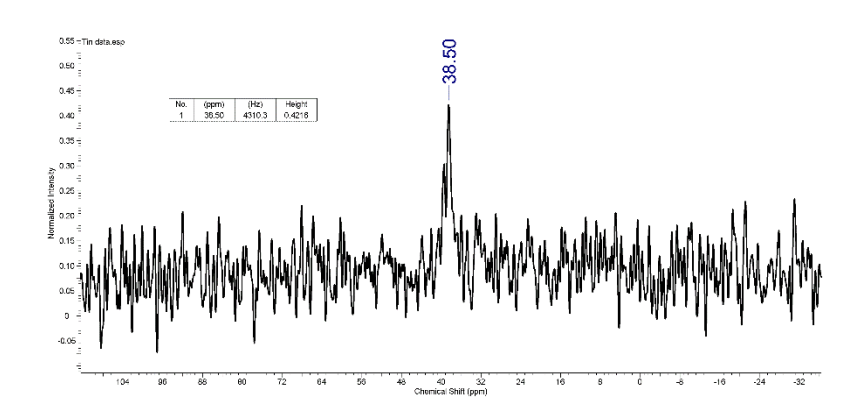
S7: Photograph of compound (1):



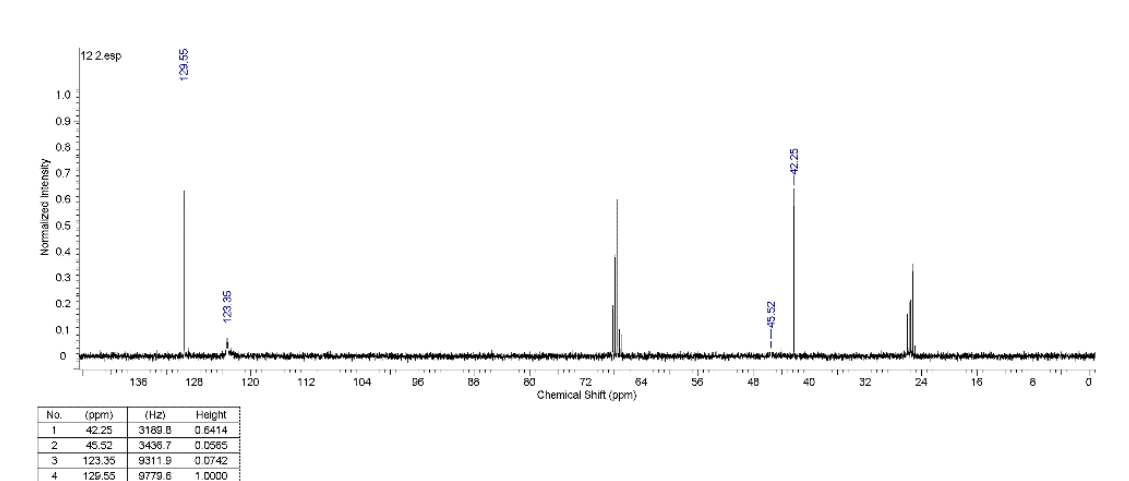
Figure S7: Picture of complex (1).

S8: 119Sn, 13C and 1H NMR Data of Compound (1):









(c)

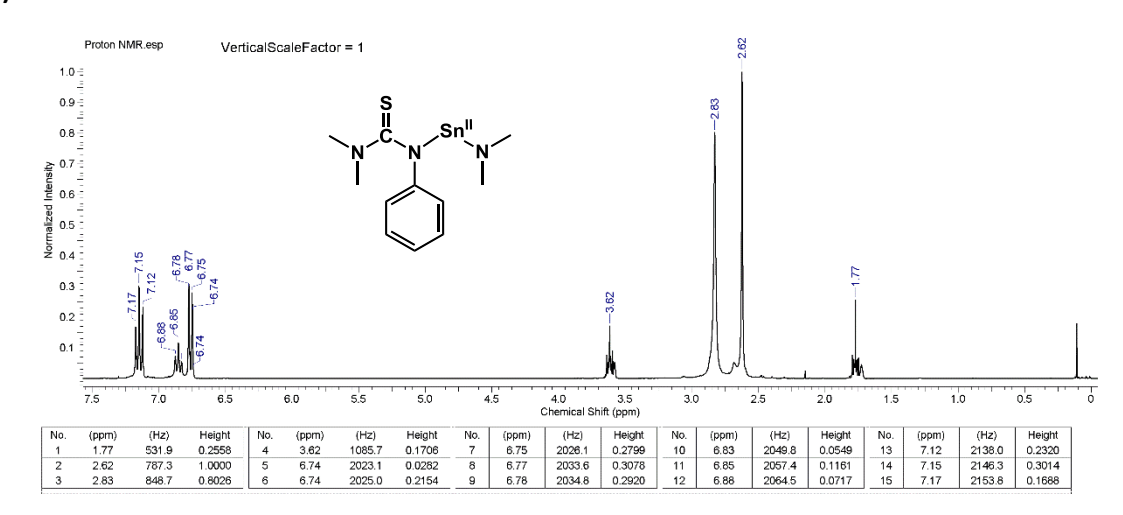
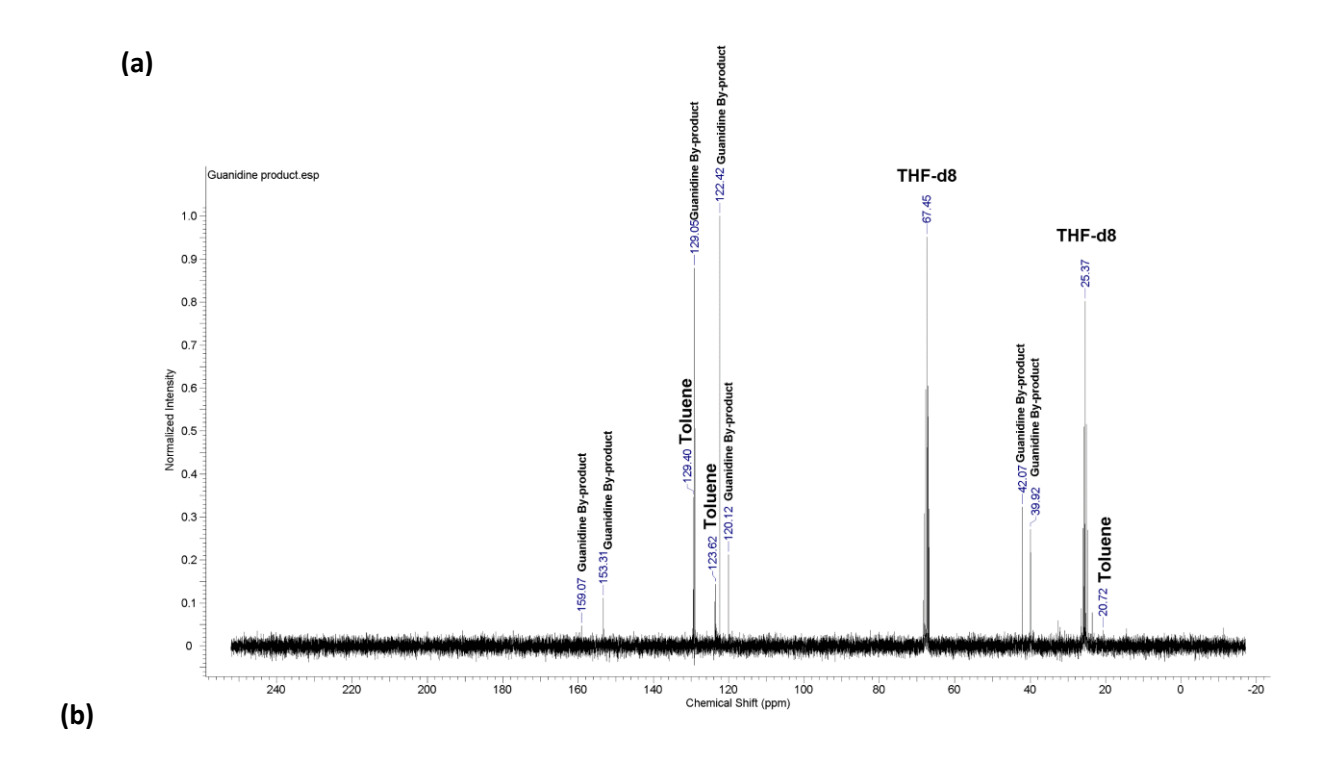


Figure S8: NMR Spectra (a)- 119 Sn NMR (111.95 MHz, THF-d8), (b)- 13 C NMR (75.5 MHz, THF-d8) and (c)- 1 H NMR (300 MHz, THF-d8) Spectrum of Compound (1).

S9: ¹³C and ¹H NMR Data for the By-Product Solution collected from the exhaust of the AA-CVD reactor:



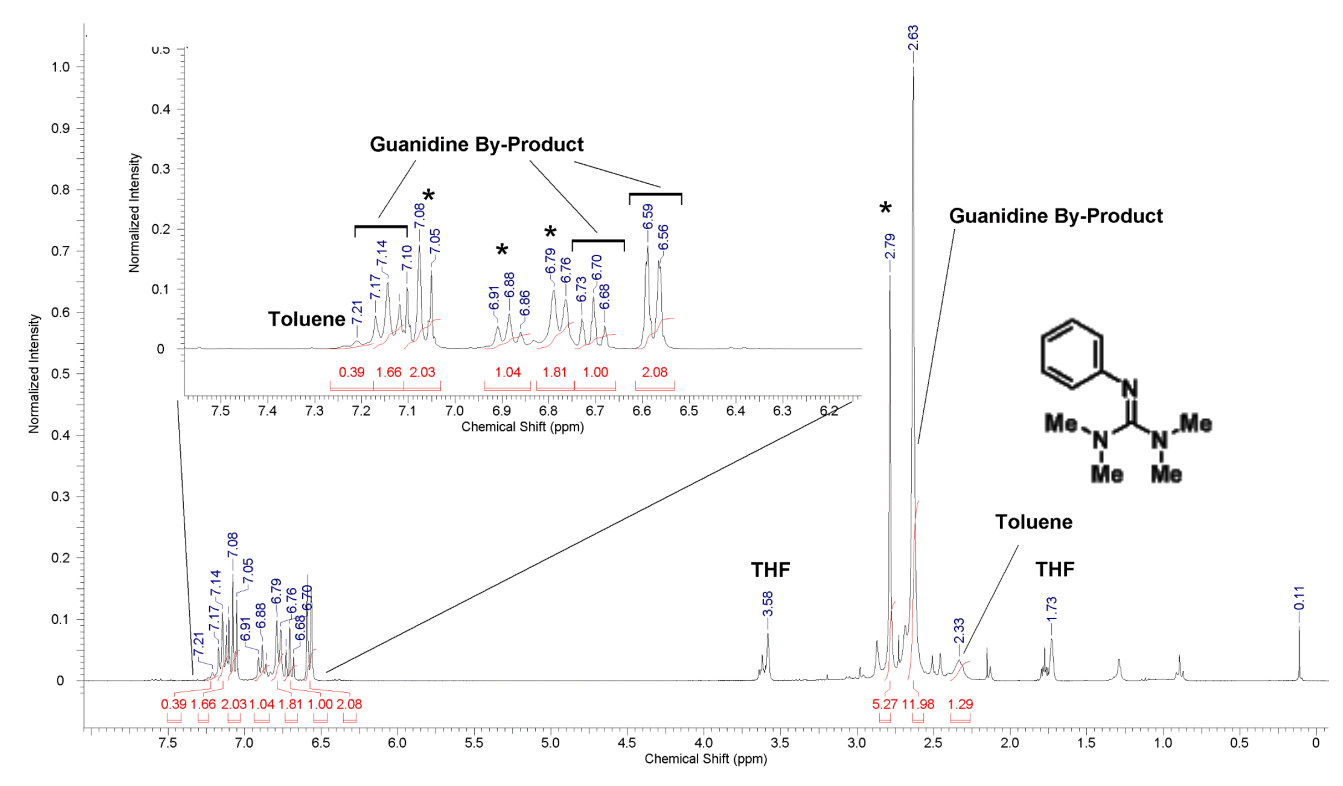


Figure S9: NMR Spectra **(a)-** 13 C NMR (75.5 MHz, THF-d8) and), **(b)-** 1 H NMR (300 MHz, THF-d8) Spectrum of the Guanidine By-Product collected from the exhaust of the AA-CVD reactor using a N_2 trap after a 40 min deposition at 375 $^{\circ}$ C. *Represent unidentifiable peaks.

Additional Characterization:

S10: Photographs of Films:



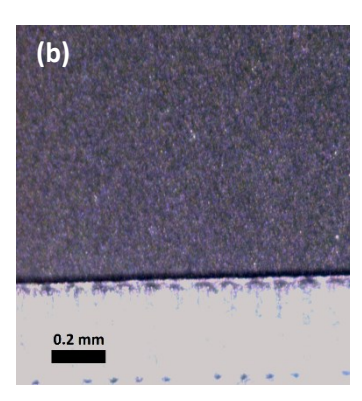


Figure S10: (a) Photograph of SnS films deposited onto FTO substrates from **1**, (a.1) at 375 °C for 40 mins and (a.2) at 300 °C for 40 mins. (b) 50 x Optical image of an α -SnS thin film deposited from **1** onto Mo substrate at 375 °C for 40 mins.

S11.: Additional SEM Images

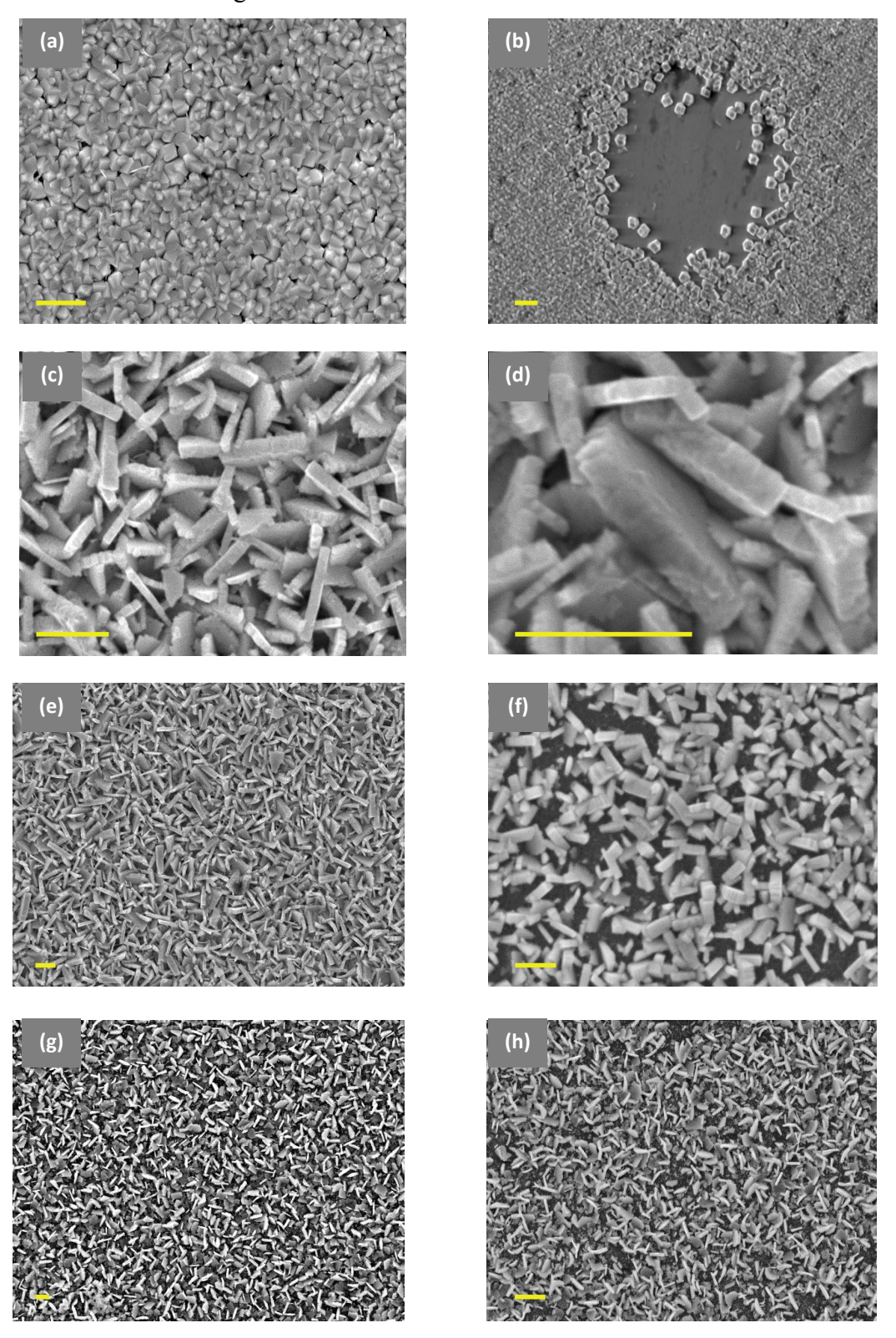


Figure S11: SEM images of SnS films deposited at different temperatures onto silicon substrates. The scale bar is set for 2 μ m. **(a,b)** ZB-SnS deposited at 300 °C, **(b)** shows an exposed region of the ZB-SnS film, **(c,d,e)** α -SnS deposited at 375 °C, **(f)** α -SnS deposited at 400 °C, **(g)** α -SnS deposited at 450 °C and **(h)** α -SnS deposited at 500 °C.

S12.	: Energy	Dispersive	e X-ray S	pectroscopy	(EDAX)	Data
O 1 = 0	• 111101 2 4	Dispersive	c_{1}	pecuoscopy	LUDIAL	Data

(a)	Precursor (1)	Sn:S	C (atm %)	O (atm %)
	300 °C (Cubic)	1:0.94	7.30 %	4.7 %
	350 °C	1:1.00	4.13 %	4.5 %
	375 °C	1:0.96	6.4 %	7.2 %
	400 °C	1:0.95	4.6 %	3.3 %
	450 °C	1:0.87	6.3 %	4.3 %

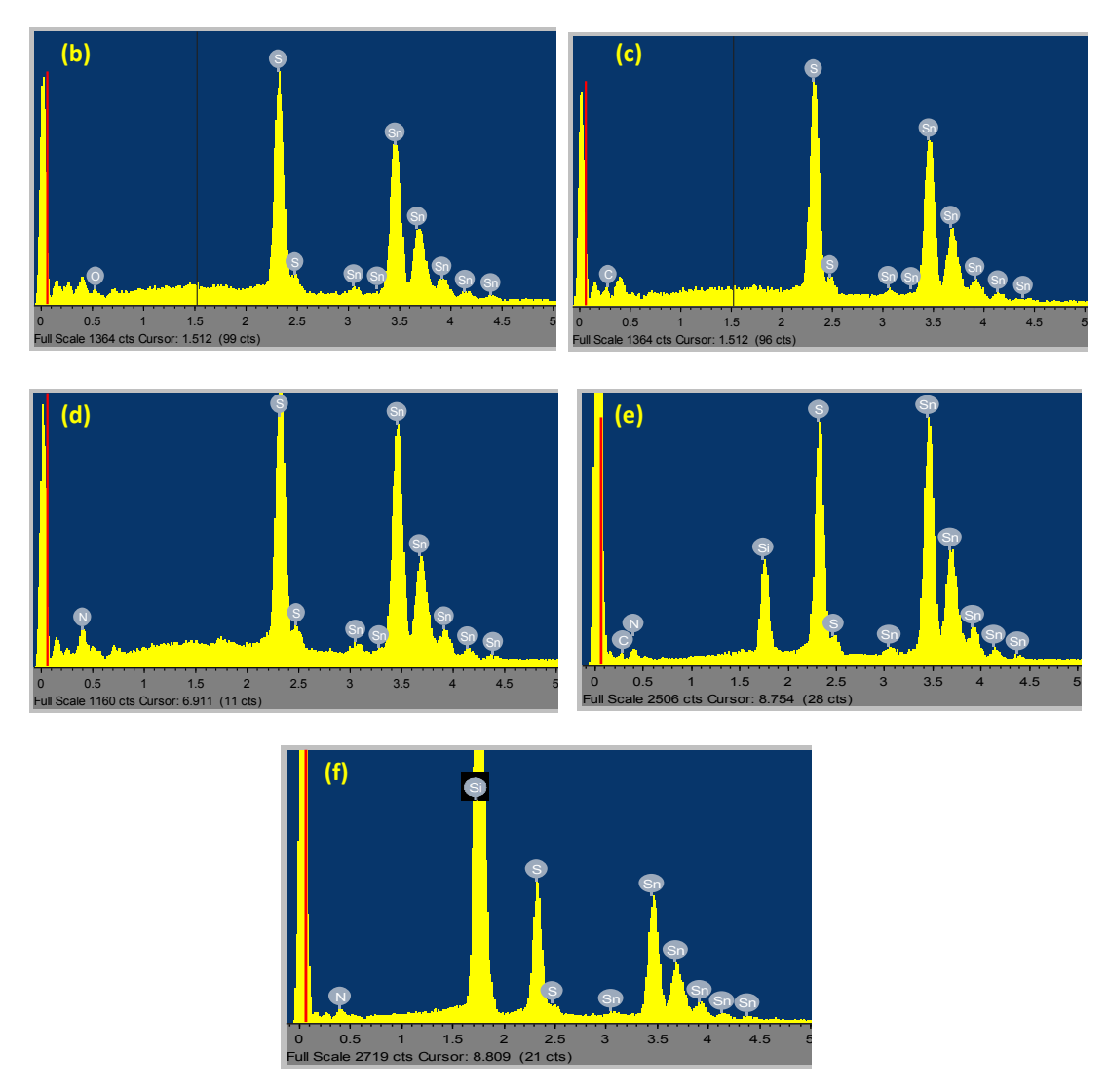


Figure S12: EDAX data for SnS films deposited onto silicon substrates using **(1)** at various deposition temperatures. **(a)** Table presenting the elemental composition for films deposited at different temperatures, presenting the atomic ratio of Sn:S, and the atomic percentage of Carbon and Oxygen. The EDAX spectra for films deposited at **(b)** 300 °C, **(c)** 350 °C, **(d)** 375 °C, **(e)** 400 °C and **(f)** 450 °C.

S13-16.: X-ray Ph

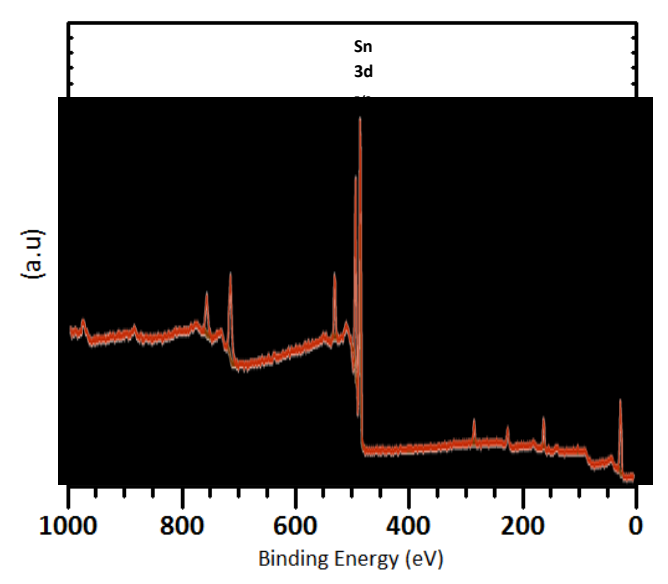


Figure S13: XPS Survey Spectrum of an un-etched α -SnS Film deposited from **(1)** at 375 °C with a deposition time of 40 mins. The same sample is used in all XPS analysis.

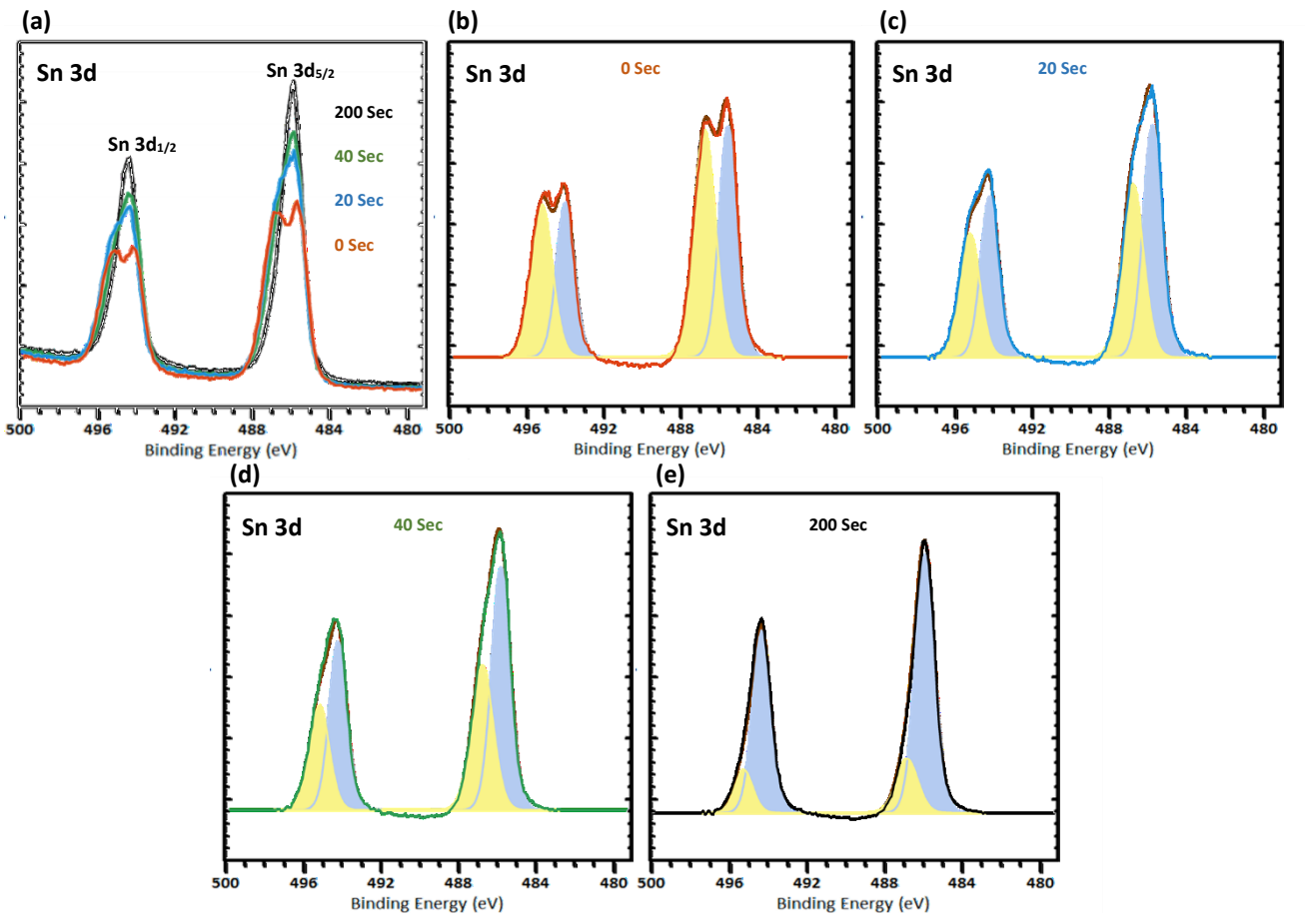


Figure S14: XPS High resolution spectra of the Sn 3d region. **(a)** Shows the normalised Sn $3d_{1/2}$ and Sn $3d_{5/2}$ peaks at consecutive etching times. **(b-e)** Normalised separate high resolution spectra after consecutive etching times, with the fitted components for binding energies representative of Sn⁺⁴/SnO₂ (yellow) at 486.9 eV (Sn $3d_{5/2}$) and 495.3 eV (Sn $3d_{3/2}$) and binding energies representative of Sn⁺²/SnS (light blue) at 486.5 (Sn $3d_{5/2}$) and 495.1 eV.

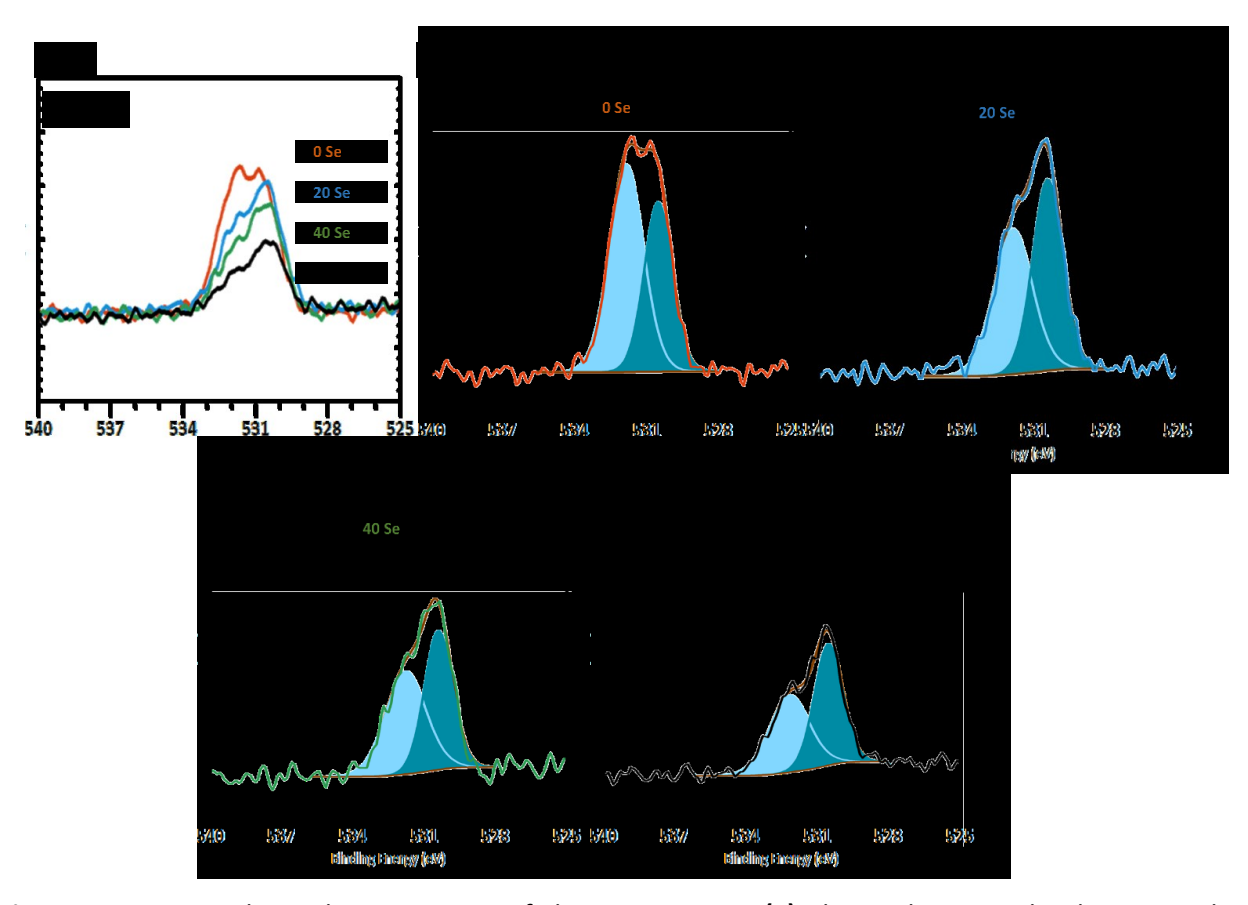


Figure S15: XPS High resolution spectra of the O 2s region. **(a)** Shows the normalised O 2s peak at consecutive etching times. **(b-e)** Normalised separate high resolution spectra after consecutive etching times, with the fitted components for binding energies representative of O-H/ Surface hydroxide groups (light blue) at 531.87 eV and for binding energies representative of SnO₂ (Dark Blue) at 530.55 eV.

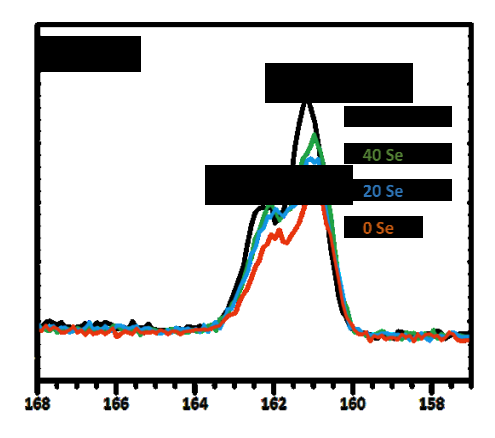


Figure S16: XPS High resolution spectra of the S 2p region, with normalised overlapping spectra collected at consecutive etching times.

S17.: Thermogravimetric Analysis (TGA) of Compound (1)

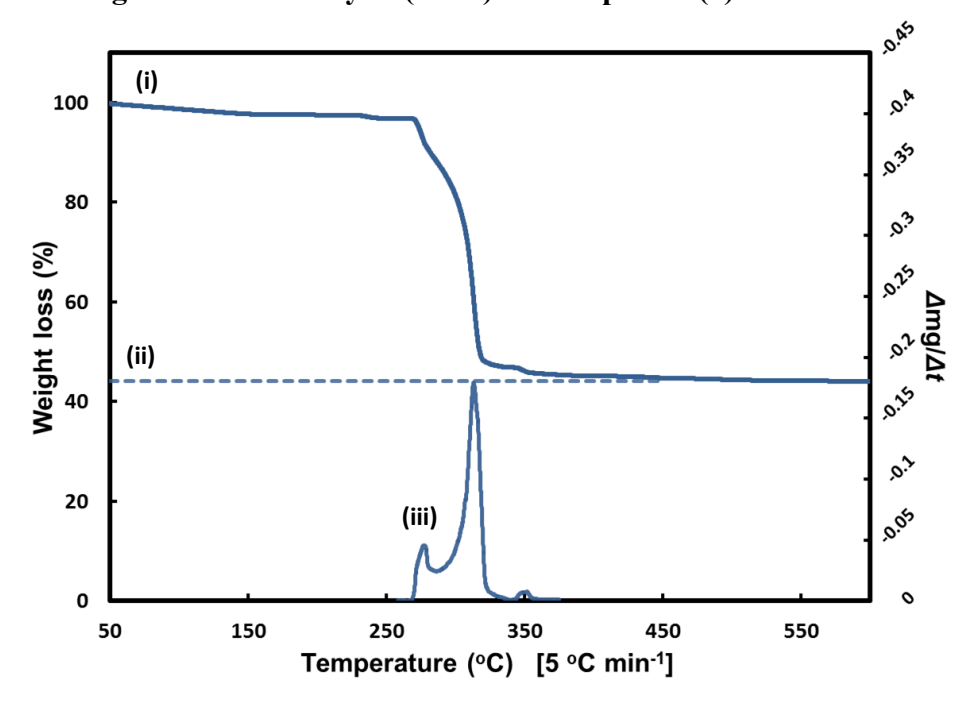


Figure S17: TGA of compound **(1)**, **(i)** the percentage mass loss with increasing temperature (at a 5 °C min⁻¹ ramp rate), **(ii)** the estimated percentage mass of compound **(1)** in order to form SnS and **(iii)** is the derivative of mass loss with respect to temperature/ time (used to identify significant mass loss events).

S18.: Optical Data

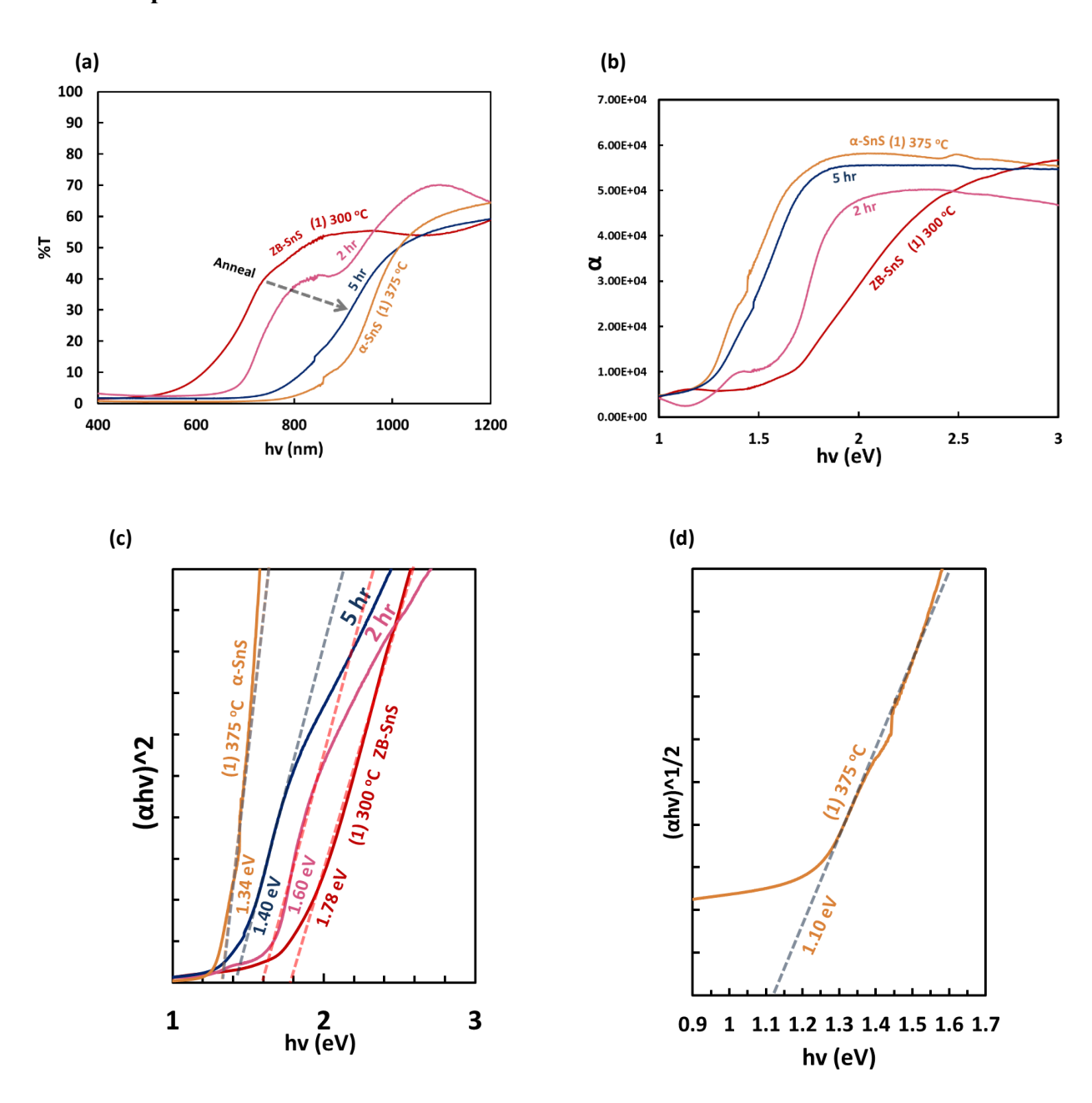


Figure S18: SnS films deposited at 300 °C (red) and 375 °C (yellow). The pink and blue spectrum of the ZB-SnS films deposited at 300 °C that have been anneal under argon at 375 °C for 2 and 5 hours, respectively. **(a)** Transmission spectrum, **(b)** Photon energy dependant absorption coefficient spectrum (calc. from $\alpha = 2.303 \text{ A/d}$) of SnS films. **(c)** Plot of $(\alpha h v)^2$ vs. photon energy (eV) used to determine the direct band gap (E_g^{direct}) of samples by extrapolating the linear region of the plot to where the y-axis = 0. Calculated E_g^{direct} of samples are presented. **(d)** Plot of $(\alpha h v)^{1/2}$ vs. photon energy (eV) used to determine the indirect band gap (E_g^{indirect}) of the α-SnS film deposited at 375 °C, by extrapolating the linear region of the plot to where the y-axis = 0, E_g^{indirect} has been calculated.

S19-20.: Photo-electrochemical and External Quantum Efficiency (EQE) Measurements

All Opto-electronic characterization was performed using samples deposited onto molybdenum substrates.

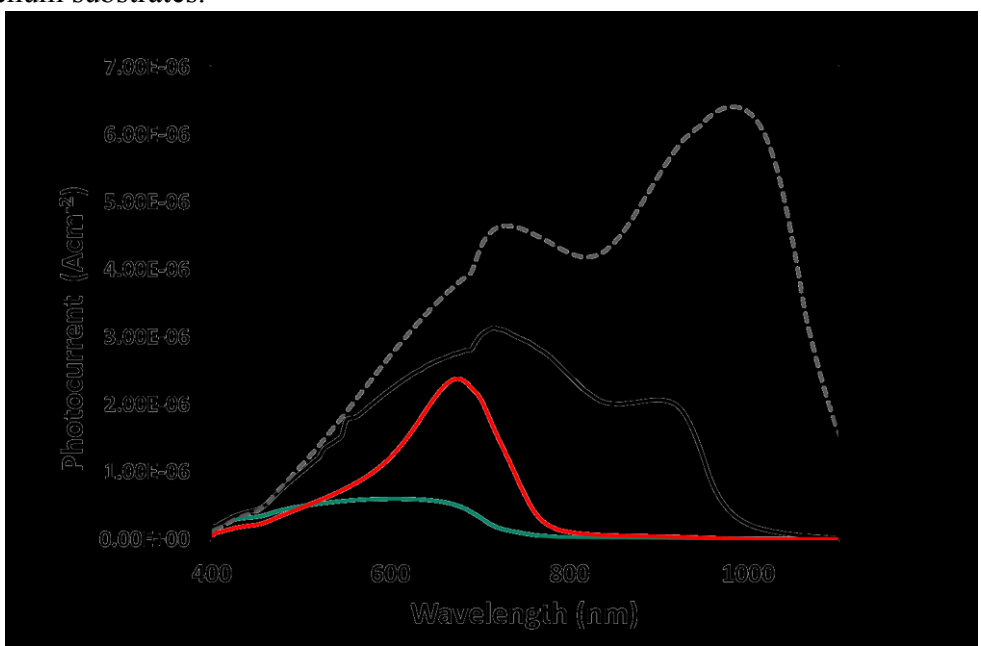


Figure S19: Photocurrent spectrum of (i) Silicon Photodiode (reference), (ii) α -SnS sample deposited at 375 °C at a bias potential of -0.7 V, and ZB-SnS sample deposited at 300 °C at a bias potentials (iii) -0.7 V and (iv) +1.0 V (vs. Ag | AgCl reference).

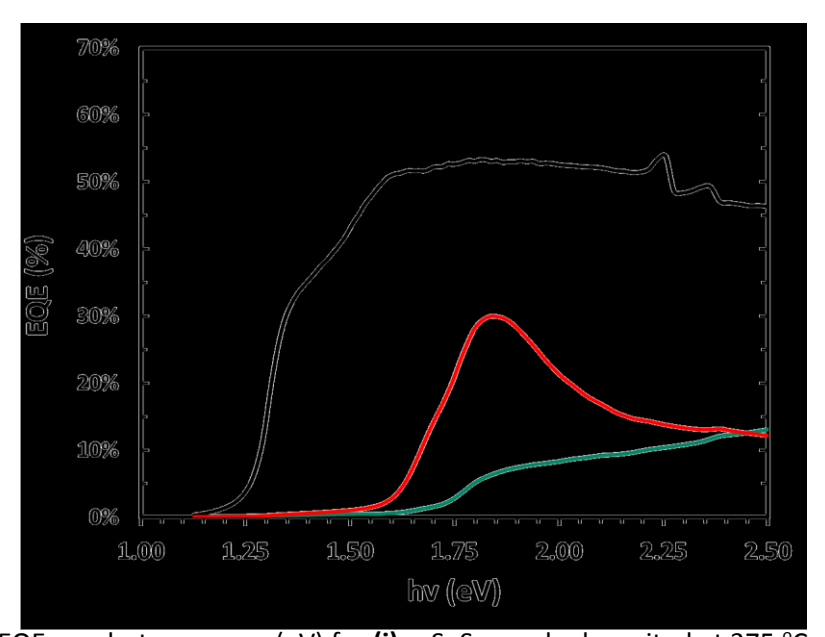


Figure S20: EQE vs. photon energy (eV) for (i) α -SnS sample deposited at 375 °C at a bias potential of -0.7 V, and ZB-SnS sample deposited at 300 °C at a bias potentials (ii) -0.7 V and (iii) +1.0 V (vs. Ag|AgCl reference).

S21-22.: Addition Powder X-ray Diffraction (PXRD) Spectrum

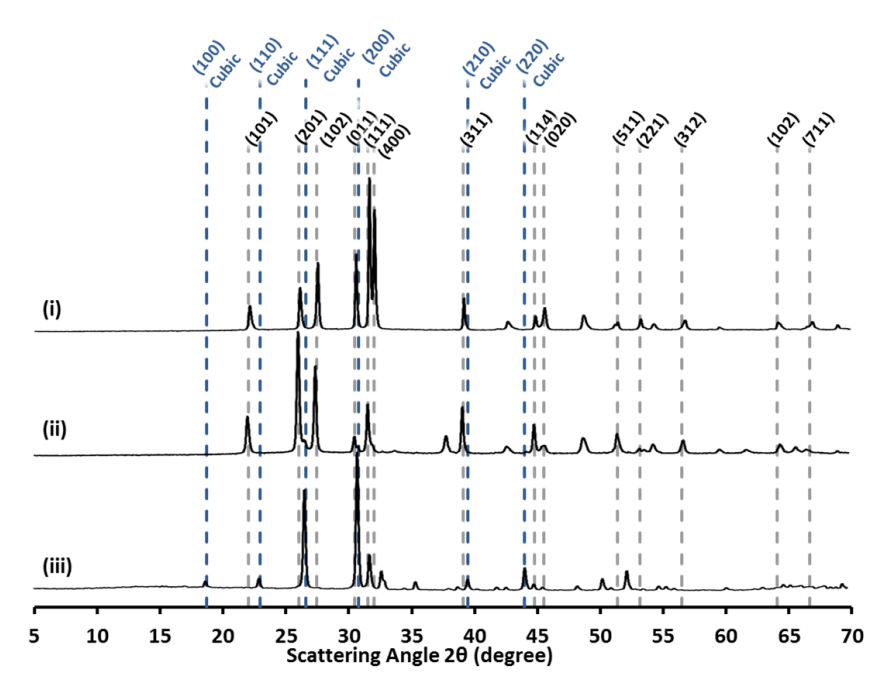


Figure S21: PXRD Specta of a ZB-SnS film deposited onto glass from (1) at 300 °C for 40 minutes. Here we examine the thermal stability of the ZB-SnS polymorph, annealing the film in an atmosphere of N_2 at 375 °C (i) for 5 hours and (ii) for 2 hours. (iii) The PXRD spectrum of the as deposited ZB-SnS film.

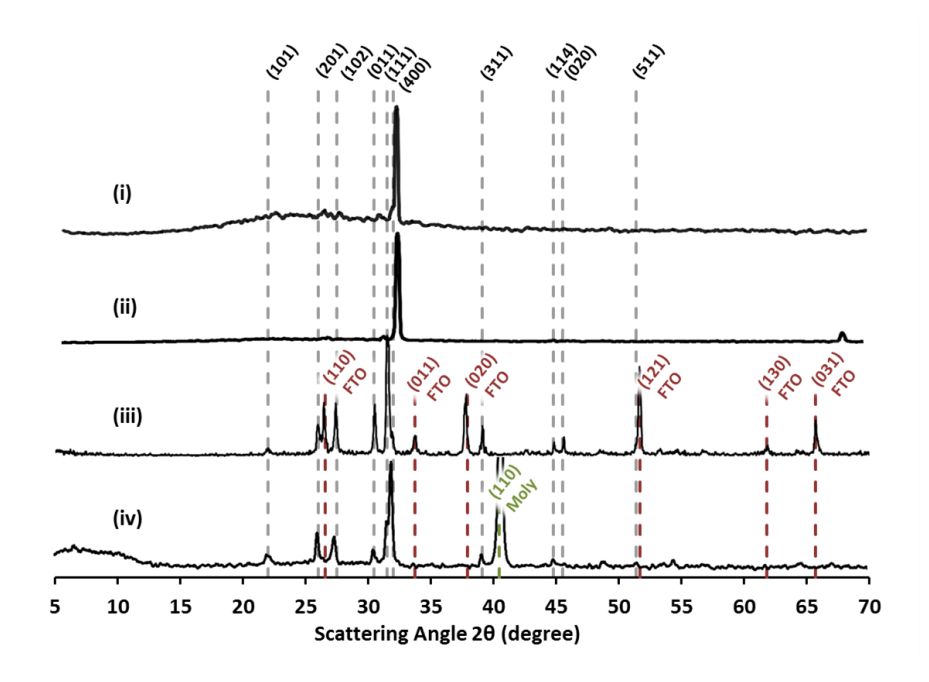


Figure S22: PXRD Spectrum of α -SnS films deposited from **(1)** at 375 °C for 40 mins onto different substrates **(i)** Si, **(ii)** glass, **(iii)** FTO, and **(iv)** Mo.

S23.: Single Crystal X-ray Diffraction Data for Compound (1)

```
CCDC identification code
                                1417256
Empirical formula
                        C<sub>22</sub> H<sub>34</sub> N<sub>6</sub> S<sub>2</sub> Sn<sub>2</sub>
Formula weight
                        684.05
Temperature 150(2) K
                0.71073 Å
Wavelength
Crystal system
                        Triclinic
Space group P-1
Unit cell dimensions a = 6.13510(10) \text{ Å}
                                                \alpha = 93.0090(10)^{\circ}.
                        b = 8.9483(2) \text{ Å}
                                                 \beta = 99.2320(10)^{\circ}.
                        c = 12.4437(3) \text{ Å}
                                                \gamma = 94.8946(16)^{\circ}.
Volume
                670.31(2) Å3
Z
Density (calculated) 1.695 Mg/m<sup>3</sup>
Absorption coefficient
                                2.040 mm<sup>-1</sup>
F(000) 340
Crystal size
                0.300 x 0.200 x 0.150 mm<sup>3</sup>
Theta range for data collection
                                        2.919 to 29.654°.
Index ranges -8 <= h <= 8, -12 <= k <= 12, -16 <= l <= 17
Reflections collected 9999
Independent reflections
                                3385 [R(int) = 0.0426]
                                        99.0 %
Completeness to theta = 25.242^{\circ}
Absorption correction Semi-empirical from equivalents
Max. and min. transmission 0.819 and 0.592
Refinement method Full-matrix least-squares on F2
Data / restraints / parameters 3385 / 0 / 149
Goodness-of-fit on F21.174
Final R indices [I>2sigma(I)] R1 = 0.0437, wR2 = 0.1103
                       R1 = 0.0467, wR2 = 0.1118
R indices (all data)
Extinction coefficient n/a
Largest diff. peak and hole 1.865 and -2.020 e.Å-3
```

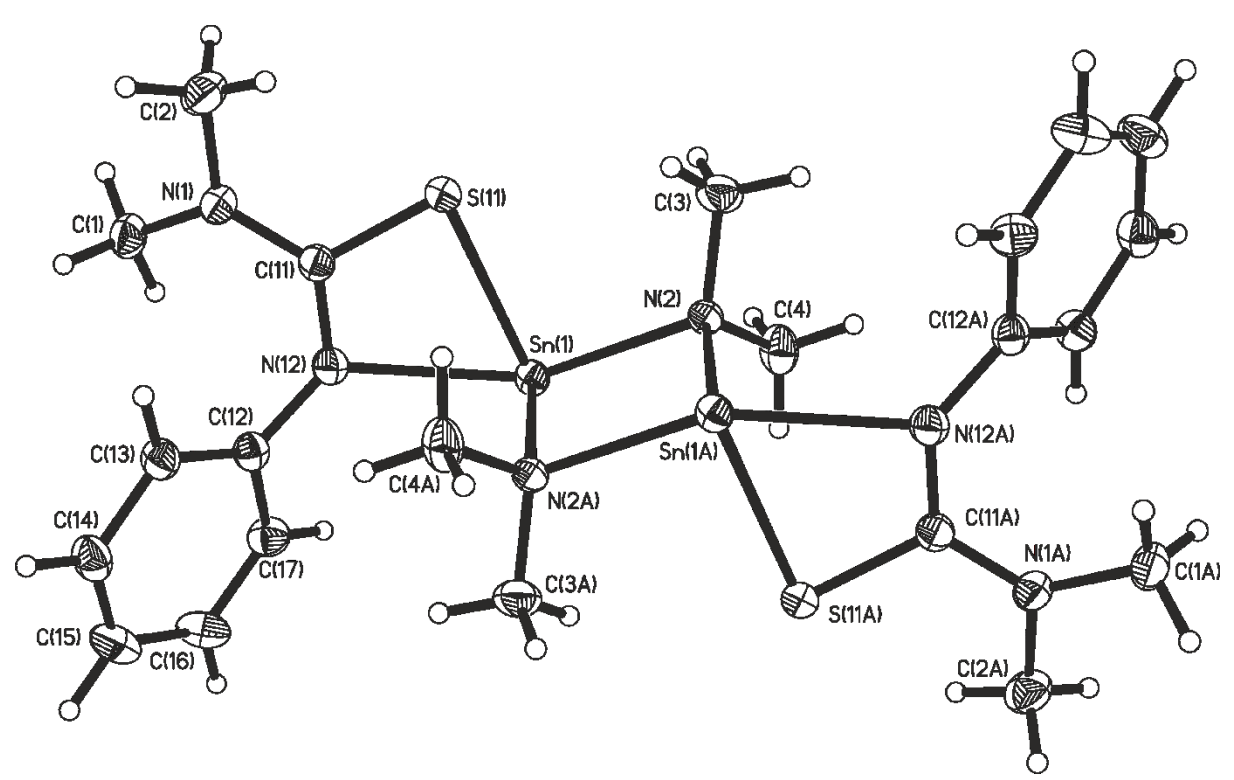


Figure S23: Single Crystal X-ray Diffraction Data for Compound (1).

References:

(1) Nelson, J., *The Physics of Solar Cells*. Imperial College Press: London, 2003; Vol. 2. (2) (a) Foley, P.; Zeldin, M., Bis(dimethylamido)tin(II). Synthesis and characterization. *Inorg. Chem.*, **1975**, 14, 2264-2267; (b) Olmstead, M. M.; Power, P. P., Structural studies of tin(II) and lead(II) dimethylamides: X-ray crystal structure of [Sn(NMe₂)₂]₂ and isolation of its lead analog. *Inorg. Chem.*, **1984**, 23, 413-415.